中國機械工程學刊第三十二卷第四期第303~312頁(民國一百年)
Journal of the Chinese Society of Mechanical Engineers, Vol.32, No.4, pp.303~312 (2011)

Application of Multi-Objective Optimization for Pollutants Emission Control in an Oil-Fired Furnace

AM. Ghasemi*, A. Saeedi** and M. Moghiman***

Keywords：*Genetic Algorithm, Furnace, NOx, soot*

ABSTRACT

This paper is aimed at the reduction of soot and NOx emissions, while maintaining reasonable temperature. For this goal, a computational model, Sprint CFD code, is incorporated with genetic algorithm (GA) to solve multi-objective optimization problem. Sprint CFD code analyzes the pollutants emissions, temperature and chemical species of the axisymmetric cylindrical furnace. An extended Genetic Algorithm called the "Non-dominating Sorting Genetic Algorithm" (NSGA-Π) is used as an optimizer thanks to its ability to derive high accurate solutions. The target purpose functions are exit temperature, NOx, and soot emissions. The design variables are air inlet axial velocity, air inlet tangential velocity, diameter of droplets and air inlet preheating. The Pareto optimum solutions obtained from Sprint-NSGA-Π are very useful to obtain optimal operational conditions. The solution shows the amount of NOx and soot emissions being kept under regulated values while the exit temperature is in the range of 1890 to 1990k.

INTRODUCTION

Oil fired furnaces are widely used in industrial applications. These high-temperature equipment utilize large amount of liquid fuel and emit many pollutants such as Nitrogen oxides (often written NOx) and soot. To meet increasing environmental concerns and more stringent emission regulation, reduction of soot and NOx emissions, while maintaining reasonable temperature become important.

There are several parameters to design and operate furnaces that have small amount of NOx and Soot while maintaining applicable temperature. But finding optimum parameters through experiments is both expensive and time-consuming. Therefore, computer simulation is a useful technique for the optimization of parameters. The optimized parameters include minimization of the amount of nitrogen oxides and soot during reasonable temperature is an interested issue for researchers [1-3]. Therefore, NOx, soot and temperature become objective function in the optimization problem. Genetic algorithms are stochastic search methods that require little information of the problem itself. It is well known that genetic algorithm have been successfully applied to many optimization problems. Extensive research has been performed exploiting the robust properties of genetic algorithms and demonstrating their capabilities across a broad range of problems [4].

Our aim in this paper is the prediction of optimum conditions in the oil fired furnace which the amount of soot and NOx emissions decrease while maintaining reasonable temperature. For this purpose, multi-objective optimization (NSGA-Π) is applied. Also, An early version of Fluent [5], Sprint CFD code, has been used for the simulations of processes inside the oil-fired furnace.

MODEL EQUATIONS

The numerical model is based on an Eulerian gas phase and a Lagrangian droplet phase formulation. Since a one-way interaction model is used for the gas flow and the droplets trajectory analysis, the air flow-field is firstly evaluated while the results are used for evaluation of the droplets trajectories.

Paper Received July, 2008. Revised February, 2009, Accepted April, 2009, Author for Correspondence: Ali Saeedi.

* *Msc of Mechanical Engineering, Department of mechanical Engineering, Ferdowsi University of Mashhad, Iran, email: Amir_m_ghasemi@yahoo.com.*

** *PhD student of mechanical Engineering, Department of mechanical Engineering, Ferdowsi University of Mashhad, Iran, email: Ali_sgn@yahoo.com.*

*** *Professor of Mechanical Engineering, Department of mechanical Engineering, Ferdowsi University of Mashhad, Iran, email: mmoghiman@yahoo.com.*

1. GAS PHASE EQUATIONS

The average gas phase equations are as follows:

Continuity:

$$\frac{\partial u}{\partial x}+\frac{1}{r}\frac{\partial}{\partial r}(rv)=\dot{m} \tag{1}$$

Momentum:

$$\frac{1}{r}\left[\frac{\partial}{\partial x}(r\rho uu)+\frac{\partial}{\partial r}(r\rho uv)\right]=-\frac{\partial p}{\partial x}+\mu\nabla^2 u-\frac{1}{r}\frac{\partial}{\partial r}(r\rho\overline{u'v'})-\frac{\partial}{\partial x}(\rho\overline{u'u'}) \tag{2}$$

$$\frac{1}{r}\left[\frac{\partial}{\partial x}(r\rho uv)+\frac{\partial}{\partial r}(r\rho vv)-\rho w^2\right]=-\frac{\partial p}{\partial r}+\mu(\nabla^2 v+\frac{v}{r^2})-\frac{1}{r}\frac{\partial}{\partial r}(r\rho\overline{v'v'})-\frac{\partial}{\partial x}(\rho\overline{u'v'})-\frac{1}{r}\rho\overline{w'w'} \tag{3}$$

$$\frac{1}{r}\left[\frac{\partial}{\partial x}(r\rho uw)+\frac{\partial}{\partial r}(r\rho vw)+\rho vw\right]=\mu(\nabla^2 w-\frac{w}{r^2})-\frac{1}{r}\frac{\partial}{\partial r}(r\rho\overline{v'w'})-\frac{\partial}{\partial x}(\rho\overline{u'w'})-\frac{1}{r}\rho\overline{v'w'} \tag{4}$$

The turbulent stresses are calculated from an algebraic stress model [6]. Also, a conventional wall-function approach is used in the near-wall region.

Energy:

$$\frac{1}{r}\left[\frac{\partial}{\partial x}(r\rho uh)+\frac{\partial}{\partial x}(r\rho vh)\right]=\Gamma_h\nabla^2 h-\frac{1}{r}\frac{\partial}{\partial r}(r\rho\overline{v'h'})-\frac{\partial}{\partial x}(\rho\overline{u'h'})+\dot{S}_h+\dot{S}_R \tag{5}$$

The energy source terms ($\dot{S}_h+\dot{S}_R$) are the energy generated due to chemical reaction and radiation. The radiation contribution to the enthalpy equation evaluated by the four flux radiation model [7]. The effect of soot, which is usually the dominant radiating species in hydrocarbon-fueled flames, on the radiative heat transfer inside the combustor is accounted by using a modified absorption coefficient (a_m) of the gas as:

$$a_m=a+b_1\rho m_S\left[1+b_T(T-2000)\right] \tag{6}$$

$$\dot{S}_h=2a\times\left[R_x+R_r-2E_b\right] \tag{7}$$

Where, R_x and R_r are the radiant fluxes which are determined by the solution of two differential equations:

$$\frac{d}{dx}\left[\Gamma_x\frac{dR_x}{dx}\right]+a(E_b-R_x)+\frac{s}{4}(R_r-R_x)=0 \tag{8}$$

$$\frac{1}{r}\frac{d}{dx}\left[r\left(\Gamma_r\frac{dR_r}{dx}\right)\right]+a(E_b-R_x)+\frac{s}{4}(R_r-R_x)=0 \tag{9}$$

The second component in the energy source term is the energy generated due to chemical reaction. The energy addition due to combustion is determined in consideration of a single step, irreversible, global reaction between the fuel vapor and oxygen following finite rate chemistry as:

$$C_{16}H_{34}+24.5O_2\rightarrow 16CO_2+17H_2O \tag{10}$$

In this study, the reaction rates that appear as source terms in species transport equations (Eq. 13) are computed by using the eddy dissipation concept [8].

$$\dot{S}_j=A\rho\frac{\varepsilon}{k}\min\left[m_F s_F, m_{Ox}\right] \tag{11}$$

The gas phase equations are completed by the ideal equation of state which determines the distribution of density as:

$$\rho=\frac{P}{RT}\left[\sum\frac{m_j}{M_j}\right] \tag{12}$$

This assumption is appropriate since the high temperatures associated with combustion generally results in sufficiently low densities, for ideal gas behavior to be a reasonable approximation.

Individual species conservation:

$$\frac{1}{r}\left[\frac{\partial}{\partial x}(r\rho um_j)+\frac{\partial}{\partial r}(r\rho vm_j)\right]=\Gamma_{mj}\nabla^2 m_j-\frac{1}{r}\frac{\partial}{\partial r}(r\rho\overline{v'm_j'})-\frac{\partial}{\partial x}(\rho\overline{u'm_j'})+\dot{S}_j \tag{13}$$

In this study, species conservation equation is solved for fuel vapor, oxygen, carbon-dioxide and soot. The conservation equation for each species contains a source term related to the chemical reaction, which is negative for fuel vapor and oxygen but positive for carbon-dioxide. The equation for fuel vapor contains an additional source term to take care of the fuel mass evaporated from the droplets.

2. LIQUID PHASE EQUATION

Evaporation and combustion of liquid fuels play an important role in producing pollutants. It is assumed that the second phase consist of spherical particles (droplets) dispersed in the continuous phase and also their contact is considered negligible due to rapid evaporation. Equations of displacement and velocity gradient in Lagrangian system for each group i of fuel particles are as follows [9, 10]:

Droplet velocity:

$$\frac{d\vec{X}_{di}}{dt}=\vec{U}_{di} \tag{14}$$

$$m\frac{d\vec{U}_{di}}{dt}=\frac{\pi}{8}D_d^2\rho_d C_D\left(\vec{U}_d-\vec{U}\right)\left|\vec{U}_d-\vec{U}\right|+m_i\vec{g}\,(\rho_d-\rho)/\rho_d+\vec{F} \tag{15}$$

Here C_D is the drag coefficient. The effect of gas phase turbulence on the droplet motion is simulated using a

stochastic approach.

Droplet mass:

$$\frac{dm^p}{dt} = -\pi\rho^2 d^2 \beta (m_{F,s} - m_F) \quad (16)$$

Droplet temperature:

$$m^d c_p^d \frac{dT^d}{dt} = \pi d^2 h (T - T^d) + \frac{dm^d}{dt}\Delta H_v \quad (17)$$

Where, ΔH_v is the enthalpy of vaporization of the liquid fuel at the droplet temperature. Mass transfer coefficient β and heat transfer coefficient h in equations 16 and 17, respectively, are evaluated from:

$$Sh = \frac{2 + 0.6\,\mathrm{Re}_d^{0.5} Sc^{0.33}}{1+B} \quad (18)$$

$$Nu = \frac{2 + 0.6\,\mathrm{Re}_d^{0.5} \mathrm{Pr}^{0.33}}{1+B} \quad (19)$$

Here B is the transfer number. Equations 15, 16 and 17 are solved for Vid, md and Td respectively, with appropriate initial conditions.

3. COMBUSTION MODELING

The energy due to combustion is determined in consideration of a single step, irreversible, global reaction between the fuel vapor and oxygen. The reaction rates that appear as source terms in species transport equations are computed by using the eddy dissipation concept [8].

NOx Modeling The thermal NOx formation mechanism proposed by Zeldovich [11] accounts for the oxidation of the nitrogen. The formation thermal NOx is highly dependent on the peak flame temperature and oxygen availability. Once oxygen atoms are formed, then oxidation of atmospheric nitrogen via the thermal NO (Zeldovich) mechanism takes place as follows:

$$O + N_2 \Leftrightarrow NO + N \quad (20)$$

$$N + O_2 \Leftrightarrow NO + O \quad (21)$$

The first reaction is generally rate controlling, since breaking the N2 bond is most difficult step in the Zeldovich mechanism. Both reactions are very important in terms of NO formation. In addition, another reaction has been proposed by Lavoie et.al [12]:

$$N + OH \Leftrightarrow NO + H \quad (22)$$

This reaction is important in fuel–rich flames and can be ignored in most fuel lean NO calculations [13]. In this study, the rate constants for forward and reverse reactions (20) and (21) were selected from the work of Hanson and Salimian [14]:

$$k_1 = 1.8*10^8 EXP\left(\frac{-38370}{T}\right) \qquad k_{-1} = 3.8\times10^7 EXP\left(\frac{-425}{T}\right)$$

$$k_2 = 1.8\times10^4 T \times EXP\left(\frac{-4680}{T}\right) \qquad k_{-2} = 3.8\times10^3 T \times EXP\left(\frac{-20820}{T}\right)$$

The NO formation rate via thermal NO mechanism is given as [15]:

$$\frac{d[NO]}{dt} = \frac{2[O]\{k_1 k_2 [O_2][N_2] - k_{-1}k_{-2}[NO]^2\}}{k_2[O_2] + k_{-1}[NO]} \quad (23)$$

At equilibrium, the rate of formation of NO is zero and the concentration of NO is found from the following equation:

$$\frac{2[O]\{k_1 k_2 [O_2][N_2] - k_{-1}k_{-2}[NO]^2\}}{k_2[O_2] + k_{-1}[NO]} = 0 \quad (24)$$

The concentrations of O_2 and N_2 are calculated in the combustion solution and [O] radical concentration can be determined by the partial equilibrium assumption [11]:

$$[O] = 36.64 \times T^{1/2} \times [O_2]^{1/2} EXP\left(\frac{-27123}{T}\right) \quad (25)$$

The prompt NO_x mechanism which first was reported by Fenimore [16] describes the reaction of the atmospheric nitrogen with hydrocarbon fuel fragments before either undergoing oxidation to NO or reduction to N_2. The prompt NO_x formation is most prominent in fuel rich regions where an abundance of hydrocarbon fragments are available. The quantities of prompt NO_x is also important in low temperature gas flames and with short time of residence. The known kinetic laws of N_2-O_2-NO system describe the growth of nitric oxide in the post flame gas, after hydrocarbons are consumed, but cannot describe a faster, transient formation of NO in primary reaction zone due to limitations by the rate of the reaction $O+N_2 \rightarrow N+NO$. The transient formation does not occur in hydrogen or carbon monoxide flames, and therefore may involve an attack of carbon or hydrocarbon radicals on nitrogen molecules. The prompt NO formation route generally accepted is as follows:

$$CH + N_2 \Leftrightarrow HCN + N \quad (26)$$

$$N + O_2 \Leftrightarrow NO + O \quad (27)$$

$$HCN + OH \Leftrightarrow CN + H_2O \quad (28)$$

$$CN + O_2 \Leftrightarrow NO + CO \quad (29)$$

From reactions 26 to 29, it can be calculated that the production of prompt NOx formation within the flame requires coupling of the NOx kinetics to an actual hydrocarbon combustion mechanism. Hydrocarbon combustion involves many complex reactions and species, they are costly to compute. Thus many investigators have proposed predictive global models to calculate prompt NO formation. In the present study,

the expression obtained by De Soete [13] is used:

$$\frac{d[NO]_{pr}}{dt} = 1.2\times10^{7}[N_2][O_2][CH_4]\exp\left(\frac{-60000}{RT}\right) \quad (30)$$

The mass transport equation is solved for the NO calculation, taking into account convection, production and consumption of NO:

$$\rho u_i \frac{\partial Y_{NO}}{\partial x_i} = \frac{\partial}{\partial x_i}\left(\rho D \frac{\partial Y_{NO}}{\partial x_i}\right) + S_{pr,NO} \quad (31)$$

The NO source term due to prompt NO_x mechanism is:

$$S_{pr,NO} = M_{NO}\frac{d[NO]_{pr}}{dt} \quad (32)$$

Where M_{NO} is the molecular weight of NO, and $d[NO]_{pr}/dt$ is computed from equation (30).

Soot Formation The emission of soot from a flame is determined by a competition between soot formation and oxidation that must be considered when a soot modeling study is carrying out. In this study, a soot model developed by Moss [17] is used. The model describes the soot formation in terms of the soot particle number density (N) and the soot particle mass density (M) and takes into account. The inception (nucleation), coagulation, growth and oxidation processes for the rates of these two model parameters are as:

$$\frac{DN}{Dt} = \left(\frac{dN}{dt}\right)_{Inception} + \left(\frac{dN}{dt}\right)_{Coagulation} \quad (33)$$

$$S_{pr,NO} = M_{NO}\frac{d[NO]_{pr}}{dt} \quad (34)$$

The acetylene inception model is used for the calculation of soot inception rate according to Brookes & Moss [18], and Moghiman et. al. [19]. Taking into account that the presence of aromatics in liquid fuels enhances inception, the inception rates are computed by:

$$\left(\frac{dN}{dt}\right)_{Inception} = c_1 N_A\left(\rho\frac{m_{C_2H_2}}{W_{C_2H_2}}\right)e^{-21100/T} \quad (35)$$

$$\left(\frac{dM}{dt}\right)_{Inception} = \frac{M_P}{N_A}\left(\frac{dN}{dt}\right)_{Inception} \quad (36)$$

Where, M_p the mass of a soot nucleus, has a value of 144 kg.kmol^{-1} based on the assumption that the soot size corresponds to 12 carbon atoms and c_1 =54 s^{-1} determined by [18].

Assuming the particles are monodispersed in size and spherical, the coagulation rate and reaction surface are given by:

$$\left(\frac{dN}{dt}\right)_{coagulation} = -\left(\frac{24R}{\rho_{Soot}N_A}\right)^{1/2}\left(\frac{6}{\pi\rho_{Soot}}\right)^{1/6}T^{1/2}M^{1/6}N^{11/6} \quad (37)$$

$$\left(\frac{dM}{dt}\right)_{growth} = c_2\left(\rho\frac{m_{C_2H_2}}{W_{C_2H_2}}\right)e^{-21100/T} \quad (38)$$

$$\times\left((\pi N)^{1/3}\left(\frac{6M}{\rho_{Soot}}\right)^{2/3}\right)$$

where R is the universal gas constant, $\rho_{soot} = 2000\,kgm^{-3}$ and c_2=9000.6 kg.m.kmol^{-1}.s^{-1} according to [20].

To predict soot oxidation the O_2-OH oxidation is used. This model includes oxidation of soot as a result of an attack by both molecular oxygen O_2 and OH radicals. As oxygen is consumed rapidly in the vicinity of the inlet port, OH-radical is an important oxidant along the combustor. More direct measurements have indicated that OH is an important oxidant of soot especially in the regions of diffusion flames where O_2 oxidation is minimal [21]. In this model, the rate of soot oxidation is given by:

$$\left(\frac{dM}{dt}\right)_{Oxidation} = -c_4\rho\eta\frac{m_{OH}}{W_{OH}}\sqrt{T}(\pi N)^{1/3}\left(\frac{6M}{\rho_{Soot}}\right)^{2/3} - c_3\rho\frac{m_{O_2}}{W_{O_2}}\exp\left(\frac{-19778}{T}\right)\sqrt{T}(\pi N)^{1/3}\left(\frac{6M}{\rho_{Soot}}\right)^{2/3} \quad (39)$$

Where η=0.13 and c_4=105.81 kg.m.kmol^{-1}.K$^{-1/2}$.s^{-1} which are obtained by converting the rate of soot mass consumption and c_3 = 8903.51 kg.m.kmol^{-1}.K$^{-1/2}$ [20].

METHOD of SOLUTION

The following assumptions have been made in the present study:

- The fuel spray is considered to consist of a finite size range, with the size distribution specified by the Rosin–Rammler function.
- A one-way interaction model is used for the gas flow and the droplets trajectory analysis. That is, it is assumed that air carries the droplets, but they have no effect on the air flow.
- Buoyancy forces are neglected.
- Effects of virtual mass force and Basset force on the droplets are not considered due to high-density ratio between the phases.
- There is no nucleation, collision, break-up, coagulation, or micro-explosion of the droplets.
- The droplets do not take part in radiative energy exchange.
- The liquid fuel is considered to be cetane ($C_{16}H_{34}$).

Numerical scheme The gas conservation equations are solved using a control-volume based computational procedure [22]. The convective terms are discretized by the power law scheme. Pressure linked equations are solved by the SIMPLE algorithm and the set of algebraic equations is solved sequentially with the line-by-line tridiagonal-matrix algorithm. The convergence criterion is determined by the requirement that the maximum value of the normalized of any equation must be less than 1×10^{-5}. Under-relaxation factor is chosen as 0.3 for all dependent variables expect nuclei and soot, for which 0.4 is suitable.

Numerical mesh A numerical mesh of 64×32 grid nodes is used after several experiments, which shows that further refinement in either direction does not change the result (maximum difference in velocity and other scalar functions in the carrier phase) by more than 2%. The grid spacing in axial and radial directions are changed smoothly to minimize the deterioration of the formal accuracy of the finite difference scheme due to variable grid spacing and in such a way that higher concentration of nodes occur near the inlet and the walls.

OPTIMIZATION by GA

A large number of problems such as oil and gas industry, engine and aircraft design can be optimized by multi-objective optimization method [23-25]. The first step in GA is the assumption of a primitive population (N_{pop}), which is resulted from arbitrary design variables. Each set of variables defines a member of a generation. The second step, based on results for objective vector, of the first generation, the same technique is employed to assign populations for next generation. The next step the crossover and mutation operations are performed. From two parent individuals, two child individuals are generated. Here, parent individuals are eliminated. Algorithm decides how to choose transcendence member from present generation to motivate the next generation. The chance devoted to each member to advance to next generation is:

$$P_i = \frac{f_i}{\sum_{j=1}^{popsize} f_i} \quad (40)$$

Where is f_i transcendence of i_{th} member in each generation. Production of each member of a generation is assumed to be a function of crossover probability Pm and mutation probability function Pc.

Followings are parameters conducting our decision making:

1) Population size
2) Generation
3) Crossover probability
4) Mutation probability
5) Selection strategy

The number of population must be high enough to achieve better selection in shorter time. However, increasing numbers of population is time consuming and decreases the rate of convergence. Due to selection strategy is stochastic process; there is no guarantee to obtain better combination of population in next generation.

In multi-objective GA, as is in our case, the aim is to find many non-dominated solutions, whose performance spread over the objective functions domain, known as Pareto solution. According to Pareto's rule, the individual A dominates the individual B if, for at least one of the objectives, A is strictly better adapted than B and if, for all other objectives, A is not worse than B. An objective is considered optimal if it is non-dominated in the sense of this rule [26, 27]. There are many algorithms of multi objective GA [28]. These algorithms are roughly divided into two groups; those are the algorithms that treat the Pareto optimum solution implicity or explicity. Most of the latest methods treat the Pareto optimum solution explicity. Typical algorithms are SPEA2 [29] and NSGA-II [30].

Constraints and limitations In MOPs, constraints and limitations are used to keep primitive variables and objectives through defined ranges. Table 1 shows limitations to keep combustion in applicable temperature.

Table1- Constraints imposed to design parameters	
Axial Velocity	[4-15] m/sec
Tangential Velocity	[4-15] m/sec
Inlet Air Temperature	[600-1000] K
Minimum diameter of fuel droplets	[10-50] µm
Maximum diameter of fuel droplets	[60-120] µm

Sprint/NSGA-II Simulation Example The Sprint CFD code can deal with several types of combustors. In the simulation, the specification of the liquid fuel combustors is summarized in Table 2.

Table2-Specification of the liquid fuel combustor	
Length	0.338 m
Diameter	0.076 m
Wall temperature	1200 K
Air inlet diameter	1.0 Cm
Fuel mass fraction	0.0005 Kg/s

The Sprint CFD code can derive several characteristics of combustors. In this simulation, exit temperature, the amount of NO_x and the amount of soot are focused.

System Construction The overview of the system is written in figure 1.

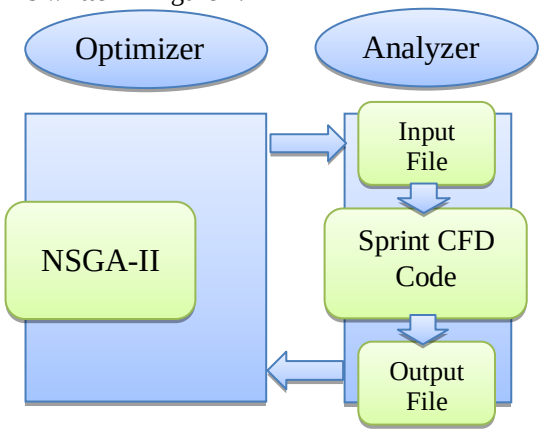

Fig. 1 overview of the system

In figure 1, the NSGA-Π is used as an optimizer and the Sprint CFD code is used as an analyzer. Between the optimizer and analyzer, text files are exchanged. Therefore, basically several types of GA and analyzer can be used in the system.

GA Parameters In this simulation, the following parameters are used. The population size is 50. The Polynomial Mutation, SBX crossover and the Tournament selection are used [30]. The crossover rate and mutation rate are 0.9 and 1/6 respectively. At the same time, both crossover distribution index and mutation distribution index are equal to 20. The simulation is terminated when the generation is over 40.

RESULTS AND DISCUSSION

SPRINT CFD Code results Numerical calculations are performed for a spray combustor of internal diameter 0.076m and length 0.338m. The computational procedure is firstly used to simulate the condition at which, inlet air temperature equals to 800K. Temperature of the walls is assumed to be at 1200K. Also, size range of the fuel droplets in spray is chosen to be in the range of 50 to 120μm.

Figure 2 shows the distribution of the gas phase velocity field within the spray combustor for the specified condition from the solution of the present numerical model. It is observed from Figure 2 that an internal recirculation zone (IRZ) is established near the central axis upstream the combustor.

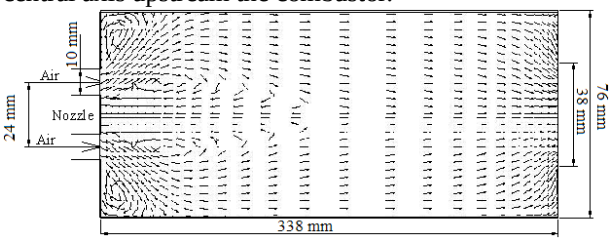

Fig. 2 The gas phase velocity field inside the combustor

That is due to the incoming swirling flow. Sudden expansion at the inlet also establishes a corner recirculation zone near the walls. Presence of the internal recirculation flow helps to stabilize the flame near the axis close to the inlet.

The accuracy of the quantitative or even the qualitative trends of the results depends on the accuracy with which velocity, temperature, and species concentration fields are determined from the numerical computation. To establish the accuracy of the present study, a possible comparison between velocity and temperature distributions predicted by the computational model is made with the experimental work of Khalil [31] under a similar condition. It is observed that the predicted axial and tangential velocity components agree fairly well with the experimental results (Figure 3)

The discrepancy between the two results can be due to turbulence modeling which shows that further works can be applied to the turbulence modeling. Similar trends can be observed from the comparison between the temperature distribution predicted by this model and the experimental results (Figure 4).

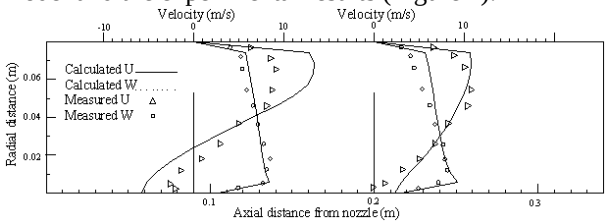

Fig. 3 Comparison of the predicted axial and tangential velocity distributions with the experimental data

The discrepancy can be attributed to the fundamental assumption made in the combustion model used (Magnussen and Hjertager model [8]) which relates the rate of combustion with turbulent energy and dissipation.

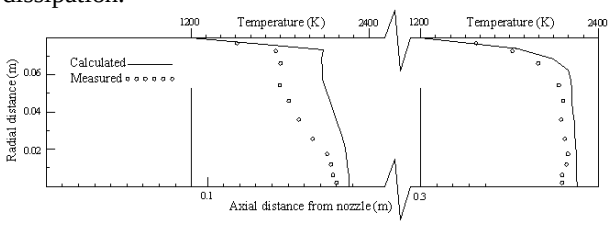

Fig. 4 Comparison of the predicted temperature with the experimental data

GA Results As it mentioned, our purpose is selection of parameters so that soot and NOx pollutants decrease and temperature maintains at the reasonable degree. Fifty Pareto optimum solutions have been derived (equal to population size) and in figure 5, optimum temperature, NOx and soot are shown. With regard to temperature, figure 5 can be divided into three zones:

1. The first zone which the temperature is lower than 1750K that has low temperature and pollutants.
2. The second one indicates high soot level and low NOx emissions that the temperature is in the range of 1750-1950K.
3. In the last zone, the temperature is more than 1950K. Soot emission is decreased; NOx emission, on the other hand, is significantly increased.

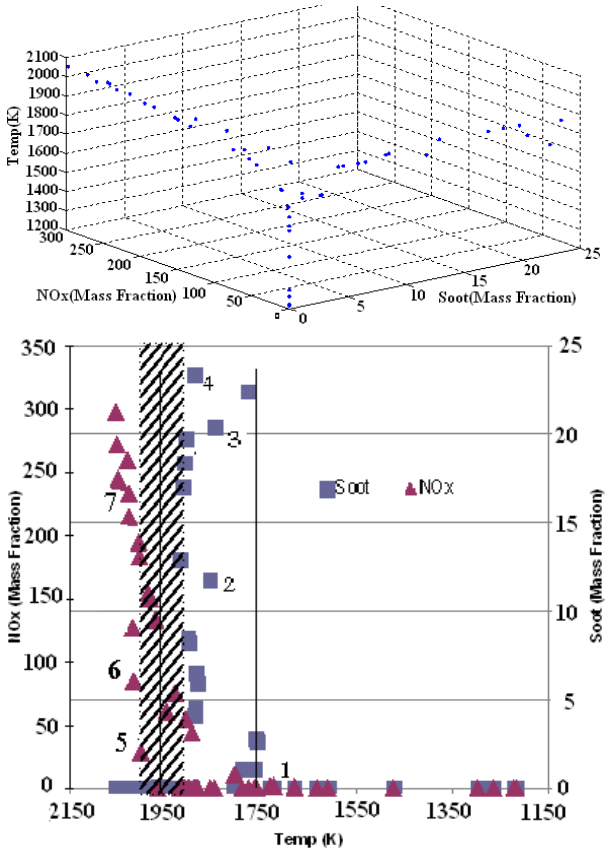

Fig. 5 Pareto optimum solutions of temperature, Soot and NOx

Seven solutions have been selected from all Pareto optimum solutions. Table 3 indicates these solutions with their conditions.

With respect to table 3, the following results are obtained:

1-The first point indicates that both temperature and pollutants are at low levels. Therefore furnace doesn't have optimum conditions. Low temperature at these conditions is as a result of high droplets diameters that cause evaporation and combustion to delay.

2-The second, the third and the fourth conditions show that temperature is in the range of 1800-1900K. These conditions display low NOx emission while soot production is high. Low NOx emission results from high soot production, because soot causes radiation heat transfer to increase. Also soot formation process is endothermic.

3-The fifth, the sixth and the seventh solutions illustrate that temperature is in the range of 1900-2100K; while soot production is negligible, NOx emission has high value.

As shown, NOx emission increases with temperature enhancement while soot emission decreases.

CONCLUSIONS

In this paper, the multi-objective optimization system is established for oil-fired furnaces. The Sprint CFD code is used to predict the emissions, temperature and chemical species of furnaces. In this simulation, temperature and the amount of NOx and Soot are minimized simultaneously by changing the air inlet axial velocity, air inlet tangential velocity, diameter of droplets and air inlet preheating. The following conclusions are reached from the analysis of the results:

- The effectiveness of the GAs and CFD code to predict the optimum conditions of the oil-fired furnace is clarified.
- For optimization of the combustion in an oil-fired furnace, multi-objective optimization should be used because of the equal importance of several objectives simultaneously.
- NOx mass fraction emission decreases with increasing soot emission.
- To have the optimum rate of pollutants emission, the temperature should be in the range 1890-1990 K.

Table 3. Operating Conditions and Pareto Solutions

	Axial Velocity (m/s)	Tangential Velocity (m/s)	Temp. inlet (K)	Fuel Rate (Kg/s)	D start µm	D last µm	Soot (ppm)	NOx (ppm)	Temp. (K)
1	13	7.5	870	0.0005	11	103	0.8	1. E-06	1680
2	6.5	12.5	820	0.0005	10	87	11	0.02	1806
3	6	13.	813	0.0005	10.5	85	20	7.3E-09	1847
4	6.5	12.5	824	0.0005	11	87	23	1.3E-08	1889
5	14	7.5	905	0.0005	16	105	1 E-05	44.5	1988
6	14	7.5	895	0.0005	12	105	0.004	94.5	2015
7	15	8	951	0.0005	13	110	0.0001	231	2054

REFERENCES

[1] Laraia, M., et al., A multi-objective design optimization strategy as applied to pre-mixed pre-vaporized injection systems for low emission combustors, Combustion Theory and Modelling, 2010, 14(2), 203-233.

[2] Saario, A., A. Oksanen, and M. Ylitalo, Combination of genetic algorithm and computational fluid dynamics in combustion process emission minimization, Combustion Theory and Modelling, 2006, 10(6), 1037-1047.

[3] Wu, J., et al., Reduction of PAH and soot in premixed ethylene-air flames by addition of ethanol, Combustion and Flame, 2006, 144(4), 675-687.

[4] Liu, F.B., A modified genetic algorithm for solving the inverse heat transfer problem of estimating plan heat source, International Journal of Heat and Mass Transfer, 2008, 51(15-16), 3745-3752.

[5] Syred, N., et al., Development of fragmentation models for solid fuel combustion and gasification as subroutines for inclusion in CFD codes, Fuel, 2007, 86(14), 2221-2231.

[6] Zhang, J., S. Nieh, and a.L. Zhou, A new version of algebraic stress model for simulating strongly swirling flows, Numerical Heat Transfer, 1992, 22, 49-62.

[7] Wang, L., et al., Interactions among soot, thermal radiation, and NOx emissions in oxygen-enriched turbulent nonpremixed flames: a computational fluid dynamics modeling study, Combustion and Flame, 2005, 141(1-2), 170-179.

[8] Magnussen, B.F. and B.H. Hjertager, On mathematical modeling of turbulent combustion with special emphasis on soot formation and combustion, Symposium (International) on Combustion, 1977, 16(1), 719-729.

[9] Basha, S.A. and K.R. Gopal, In-Cylinder Fluid Flow,turbulence and spray models—A review, Renewable and Sustainable Energy Reviews, 2009, 13, 1620-1627.

[10] Xia, J.L., et al., Numerical and experimental study of swirling flow in a model combustor, Journal of Heat and Mass Transfer, 1998, 41(11), 1485-1497.

[11] Warnatz, J., U. Mass, and R.W. Dibble, Combustion,Physical and Chemical Fundamentals, Modeling and Simulation, Experiments, Pollutant Formation. 4th Edition ed, 2006, Springer.

[12] Lavoie, G.A., j.B. Heywood, and J.C. Keck, Experimental and theoretical investigation of nitric oxide formation in internal combustion engines, Combustion Science Technology, 1970, 1, 313.

[13] Soete, G.G.D., Fundamental chemistry of NOx and N2O formation and destruction, Lecture 6, Third flame research coarse, IFRF, The Netherlands, 1990.

[14] Hanson, R.K. and S. salimian, Survey of Rate Constants in H/N/O System, in Combustion Chemistry, W.C. Gardiner, Editor, 1984.

[15] NOx Post-processor user manual, in Fluent Version 6, 2004.

[16] Fenimore, C.P., Formation of nitric oxide in premixed hydrocarbon flames, Symp. (Int.) on Combustion, The Combustion Institute, 1971, 373-381.

[17] Moss, J.B., C.D. Stewart, and K.J. Young, Modeling soot formation and oxidation in a high temperature laminar diffusion flame burning under oxygen-enriched conditions, Combustion and Flame, 1995, 101, 491-500.

[18] Brookes, S.J. and J.B. Moss, Predictions of soot thermal radiation properties in confined turbulent jet diffusion flames. Combustion and Flame, 1999, 116, 486-503.

[19] Moghiman, M., et al., Measurements and modeling of soot and CO pollutant emissions in a large oil fired furnace, The Arabian Journal for Science and Engineering, 2009, 34(2B).

[20] Wen, Z., et al., Modeling soot formation in turbulent kerosene/air jet diffusion flames. Combustion and Flame, 2003, 135, 323-340.

[21] Beltrame, A., et al., Soot and NO formation in methane–oxygen enriched diffusion flames, Combustion and Flame, 2001, 124, 295-310.

[22] Versteeg, H.K. and W. Malalaseke, An introduction to computational fluid dynamics-The finite volume method, 1996, Longman Scientific & Technical.

[23] Weigang, A. and L. Weiji, Interactive Multi-objective Optimization Design for the Pylon Structure of an Airplane, Chinese Journal of Aeronautics, 2007, 20(6), 524-528.

[24] Sayyaadi, H., E.H. Amlashi, and M. Amidpour, Multi-objective optimization of a vertical ground source heat pump using evolutionary algorithm, Energy Conversion and Management, 2009, 50(8), 2035-2046.

[25] Khosla, D.K., S.K. Gupta, and D.N. Saraf, Multi-objective optimization of fuel oil blending using the jumping gene adaptation of genetic algorithm, Fuel Processing Technology, 2007, 88(1), 51-63.

[26] Van Veldhuizen, D.A. and G.B. Lamont, Multiobjective evolutionary algorithms: analyzing the state-of-the-art, Evolutionary computation, 2000, 8(2), 125-147.

[27] Kahrom, M., S.M. Javadi, and P. Haghparast, Apllication of Multi Objective Genetic Algorithm to Optimize Heat Transfer Enhancement from a Flat Plate, International Review of Mechanical Engineering (I.RE.M.E.), 2010, 4(2), 167-175.
[28] Zheng, L.-G., et al., A comparative study of optimization algorithms for low NOx combustion modification at a coal-fired utility boiler, Expert Systems with Applications, 2009, 36(2, Part 2), 2780-2793.
[29] Wei, Z., et al., Research on quality performance conceptual design based on SPEA2+, Computers & Mathematics with Applications, 2009, 57(11-12), p. 1943-1948.
[30] Deb, K., et al., A Fast and Elitist Multiobjective Genetic Algorithm: NSGA-II, IEEE transactions on evolutionary computation, 2002, 6(2), 182-197.
[31] Fricker, N., Modelling of Furnaces and Combustors: E. E. Khalil, Abacus Press, International Journal of Heat and Mass Transfer, 1985, 28(6), 1241-1241.

NOMENCLATURE

A	pre-exponential rate constant
a	absorption coefficient
a_m	modified absorption coefficient
B	transfer number
b_1	empirical coefficient
b_T	empirical coefficient
C_p	specific heat
C_D	Drag coefficient
d, D	droplet diameter
h	enthalpy in Eq. (5) and heat transfer coefficient in Eq. (17)
M	molecular weight
m	Mass fraction
$m_{f,s}$	fuel vapor mass fraction at the particle surface
Nu	Nusselt Nubmer
P	Pressure
Pr	Prandtl number
R	Gas phase constant
r	radial direction
Re_d	droplet Reynolds number
s	stiochiometric coefficient. Eqs. (11) & scattering coefficient. [Eqs. (8,9)]
Sc	Schmidt number
Sh	Sherwood number
T	temperature
U	Velocity
U,v,w	Axial, radial and swirl velocities
u',v',w'	fluctuating components of gas velocities
x	axial direction

Greek symbols

β	empirical coefficient
Γ	diffusion coefficient
ε	rate of dissipation of the kinetic energy
μ	dynamic viscosity
κ	kinetic energy of turbulence
ν	kinematic viscosity
ρ	density

Subscript

d	droplet
g	Gas phase
O_x	oxygen
d	droplet
f	fuel vapor

Superscript

d	droplet
p	droplet

應用多目標最佳化於燃油爐內汙染物排放之控制

AM. Ghasemi , A. Saeedi , M. Moghiman
馬什哈德菲爾多西大學機械工程學系

摘 要

這篇論文主要目的在探討當維持合理的溫度下，煤煙與 NOx 排放量的減少行為。文中採用 Sprint CFD code 建立此問題的計算模型，並結合遺傳算則(GA)來求解此多目標最佳化問題。利用 Sprint CFD code 分析軸對稱圓柱型熔爐中汙染物的排放量、溫度以及化學組成，而一種名為”非優勢排序遺傳演算法”（NSGA-Ⅱ)的延伸性遺傳算則被用來做為求解此問題的最佳化工具，藉由此工具，可得到問題之高精度解。訂定目標函數為出口溫度、NOx 與煤煙的排放量，設計參數為入口空氣的軸向速度、切向速度、液滴的直徑以及入口空氣的預熱，藉由 Sprint-

NSGA-Ⅱ 可求得最佳的操作條件。而從結果可得知，當出口溫度在 1890~1990K 的範圍之間，NOx 與煤煙的排放量可保持在標準值之下。